PCCP

Structural variations in self-assembled monolayers of 1-pyrenehexadecanoic acid and 4,4′-bipyridyl on graphite at the liquid–solid interface

Hiroshi Uji-i, Masahito Yoshidome, Jonathan Hobley, Koji Hatanaka and Hiroshi Fukumura*

Department of Chemistry, Graduate School of Science, Tohoku University, Sendai, 980-8578, Japan. E-mail: fukumura@orgphys.chem.tohoku.ac.jp; Fax: 81 22 217 6570; Tel: 81 22 217 6567

Received 19th June 2003, Accepted 21st August 2003
First published as an Advance Article on the web 5th September 2003

Static and dynamic structures in self-assembled monolayers containing 1-pyrenehexadecanoic acid (PHDA) at a liquid–solid interface were investigated with scanning tunneling microscopy. Uni-component adsorption layers made a specific structure having ring figures corresponding to pyrene groups, whereas the co-adsorption of PHDA and 4,4′-bipyridyl resulted in two different structures depending on their concentrations and the ambient temperature. When the concentration of 4,4′-bipyridyl was high and the temperature at around 290 K, a dynamic bistable structure was observed within a stacked row of molecules without causing any disorder to the assembly as a whole. The bistability is considered to be due to molecular desorption–adsorption process occurring at the anti-parallel configuration of two neighbouring PHDA molecules.

Introduction

Scanning tunneling microscopy (STM) has considerably contributed to revealing the nature of physisorbed organic molecules at liquid–solid interfaces. Not only the static properties,[1] such as functionality,[2,3] chirality,[4,5] but also dynamic processes related to deposition–adsorption[6–15] have been studied. Recently, several reviews have been presented summarizing the usefulness of STM for investigating a variety of organic molecules at interfaces.[16–21] From the viewpoint of deposition–adsorption dynamics, phenomena observed to date can be classified into two classes, namely, processes approaching to thermodynamically stable states and natural fluctuations existing in equilibrated systems.

Crystal growth is one example of processes directed towards the condition of minimizing free energy, which means that the overall dynamics appear to be one-way. The motion of individual molecules is too fast to be observed with a conventional STM, whose time resolution is generally of the order of seconds. However, collective motion of molecules can be visualized over nanometer ranges. Stabel *et al.* investigated the self-assembled monolayers of alkylated octathiophene derivatives at the solution–graphite interface.[8] Small domains in the monolayers were overtaken by large domains and eventually disappeared, as expected from the Ostwald ripening process, which explains domain growth by reduction of the interfacial potential energy. Dynamic processes in two component monolayers have also been studied. Hibino *et al.* investigated mixtures of fatty acids having alkyl chains of different lengths.[9,10] They found that molecular motion within monolayers often occurred at the liquid–solid interface and adsorption of fatty acids with longer alkyl chains was preferential.[10] Gesquiere *et al.* observed the dynamics in the self-assembled monolayers of isophthalic acid derivatives with a speed of two frames per second and found that non-fluorinated molecules progressively replaced the fluorinated molecules.[11] These dynamic processes were always initiated at the domain boundary due to the local instability of adsorption.

Fluctuation dynamics in physisorbed monolayers apparently occurring without rearrangement of whole monolayers have also been reported. Stabel *et al.* observed "fuzzy" images of alkylated anthraquinone derivatives within loosely packed monolayers, the cause of which was attributed to the significantly large free volume.[12] Padowitz *et al.* investigated the exchange process between alkylated ether and thioether in monolayers with the compounds in solution.[13,14] The residence time of the thioether molecules in the monolayers depended on the neighbouring adsorbates owing to differences in the weak intermolecular interactions. Cousty *et al.* also observed monolayer structures formed with binary mixtures of *n*-alkanes and found point defects due to the insertion of short alkanes amongst long alkane molecules.[15] These structural fluctuations were found to occur randomly but never induced co-operative molecular motion leading to a large-scale fluctuation within the assembly.

In this article, we report apparent domino-like molecular reorientation in self-assembled monolayers of 1-pyrenehexadecanoic acid (PHDA) and 4,4′-dipyridyl (4Bpy). We found that a single defect propagated itself over 10 molecules, enlarging the fluctuation region due to co-operative molecular motion. Since π–π interaction affects the crystal structure of large aromatic moieties, *e.g.* pyrene and perylene, it is expected to influence desorption and adsorption dynamics through similar interactions. The present STM images showed that these molecules formed a bistable structure, casting a new light on fluctuation modes in the crystal.

Experimental section

PHDA was purchased from Molecular Probes, 4Bpy from Tokyo Kasei, and 1-phenyloctane from Aldrich. All reagents were used without further purification. In the present experiment, two kinds of solutions were prepared. PHDA (**1**) and mixtures of PHDA and 4Bpy (**2**) were made up in concentrated but unsaturated solutions of 1-phenyloctane. Physisorbed

self-assembled monolayers were obtained by depositing a drop of the solution on a basal plane of highly oriented pyrolytic graphite (HOPG: NT-MDT, grade ZYH) and the STM tip was immersed in this solution. The static and dynamic phenomena of monolayers were investigated with an STM (SOLVER P-47 STM, NT-MDT) *in situ* at the liquid–solid interface. The STM tip was a mechanically cleaved Pt/Ir (8 : 2) wire. STM measurements were carried out at the temperature range from 290 to 295 K with an accuracy of ± 1 K, which was monitored throughout the experiment. The constant current mode and the constant hight mode were, respectively, employed for investigating the static properties of the self-assembled monolayers and for imaging dynamic processes in the monolayers. The latter mode allowed us to scan interfaces with a high speed.

Results and discussions

Self-assembled monolayers of PHDA were formed with stable single 2D-crystalline domains as large as a few thousand nm^2 on graphite. Fig. 1a shows a typical STM image of self-assembled monolayers of PHDA taken over a scan area of 12×12 nm^2. The bright rings in the image correspond to the aromatic moieties, *i.e.*, the pyrene groups of the molecules. The alkyl chains were observed as the darker rows. At the darkest areas the carboxyl groups are known to form hydrogen bonds.[9] The PHDA molecules are fully interdigitated and make a close packed structure (Structure I). The plane of the pyrene unit is deduced to be oriented nearly parallel to the graphite surface, since individual pyrene rings were clearly observed in the image. The distance between adjacent alkyl chains was about 0.45 nm and their long axes were parallel to the graphite axis. Therefore it is deduced that the alkyl chains are aligned with their zigzag plane parallel to the graphite surface, as reported before.[1] In the monolayers, the length of the alkyl chain plays an important role. Since the length is almost the same as the size of the neighboring two pyrene units, PHDA can fully interdigitate and form a stable assembly. A proposed space-filling model is shown in Fig. 1b.

Fig. 2 shows calculated molecular orbitals of alkylated pyrene. Whereas the total electron density of pyrene extends all over the molecule (data not shown), the electron densities of the HOMO and the LUMO levels are low at the center of the pyrene unit. Therefore the tunneling process was deduced to relate to molecular orbital around the HOMO or the LUMO levels, because the pyrene groups were observed as bright rings in the STM image. Although the orientation between the pyrene unit and the underlying graphite is different with respect to the lateral position due to the mismatch between the lattice of the molecular assembly and the graphite, every pyrene unit was observed with the same contour in the STM image. This result is in contrast to a previous report on a perylene derivative observed in ultra high vacuum.[22] The contrast of molecular images was found to depend on the molecular orientation and the position on graphite. Ogawa *et al.* calculated the partial electron density for several orientations of the perylene derivative adsorbed on the underlying graphite lattice.[23] They concluded that the contrast modulation of the molecular image coincides with the distance between the center of the adsorbed molecule and the nearest carbon atom of the graphite. The probable reasons why the contrast modulation was not observed in our system are that the adsorbed molecules may fluctuate at the liquid–solid interface at room temperature or the pyrene units may be slightly tilted with respect to the graphite surface owing to preferential affinity between the long alkyl chains and the substrate.

The monolayers from the mixture of PHDA and 4Bpy solution had structures that were quite different from unicomponent monolayers. Fig. 3a shows an STM image of the

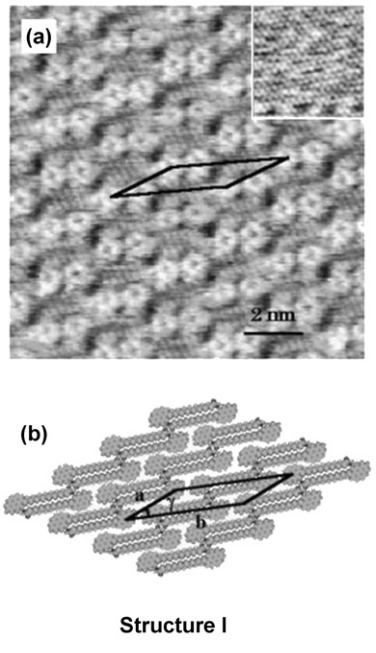

Fig. 1 (a) An STM image of 1-pyrenehexadecanoic acid on HOPG (Structure I) scanned over a 12×12 nm^2 area. (Bias voltage: 0.8 V (sample negative), tunneling current: 0.15 nA, with the constant current mode.) The inset in (a) is an STM image of the underlying graphite substrate (bias voltage: 0.1 V (sample negative), tunneling current: 0.15 nA, with the constant current mode). (b) Space-filling model of 1-pyrenehexadecanoic acid (Structure I). The parameters of the unit cell are $a = 2.11 \pm 0.05$ nm, $b = 3.91 \pm 0.05$ nm, $g = 23.5 \pm 2°$. The number of molecules per unit cell is two.

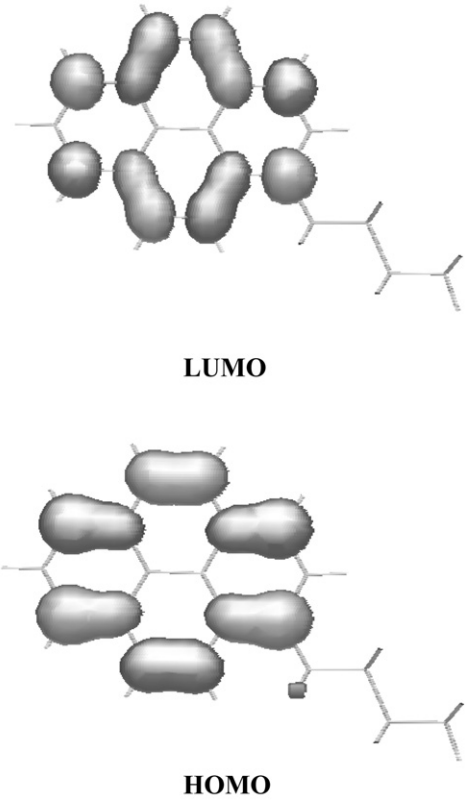

Fig. 2 Charge density calculated with PM3 molecular orbitals of the alkylated pyrene derivative. Top: the lowest unoccupied molecular orbital (LUMO), bottom: the highest occupied molecular orbital (HOMO).

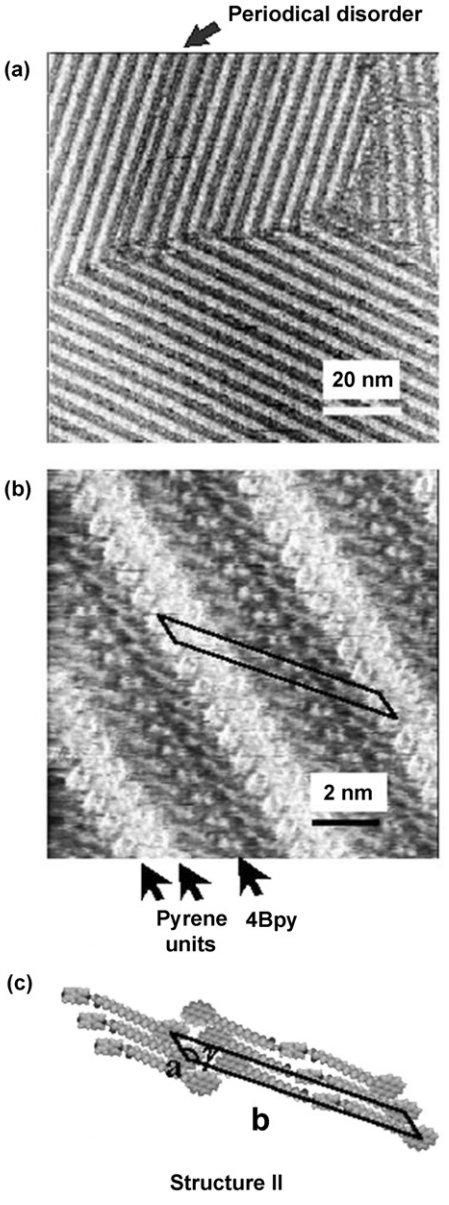

Fig. 3 (a) An STM image of 1-pyrenehexadecanoic acid and 4,4′-bipyridyl on HOPG. The scanning area is 150×150 nm^2. (b) A higher resolution STM image of the monolayers over a 12×12 nm^2 area (bias voltage: 1.0 V (sample negative), tunneling current: 0.35 nA, with the constant current mode). (c) Space-filling model of 1-PHDA and 4Bpy (Structure II). The parameters of the unit cell are $a = 0.85 \pm 0.05$ nm, $b = 7.20 \pm 0.05$ nm, $g = 130 \pm 5°$. The number of molecules per unit cell is two 1-PHDA and one 4Bpy.

two-component monolayers that was taken with a large scan area of 100×100 nm^2. PHDA molecules co-adsorbed with 4Bpy on graphite and formed a stable assembly. In the STM image, domain boundaries were often observed. The co-adsorbed monolayers formed domains smaller than the uni-component monolayers did. Interestingly, periodical disorders within the 2D crystal were sometimes observed within a single domain, as indicated with an arrow in the image. These were observed only at the lower temperatures achievable with our experimental system (290 ± 1 K). Further, these disordered structures were only observed when the concentration of PHDA was 10^{-4} M and that of the 4Bpy was in the range from 10^{-1} M to 10^{-2} M. On the other hand, the ordered structure appeared at all measurable temperatures when the PHDA and 4Bpy concentrations were 10^{-4} M and 10^{-3} M, respectively. At around 290 K, the disordered structure was continuously observed for more than a few hours. On the other hand, at higher temperatures (around 293 K) these periodical disorders were not observed as stable systems probably because they quickly changed their structure to the ordered structure during scanning.

Fig. 3b shows a higher resolution STM image of the area that was constructed with the ordered packing structure (Structure II). In this area, PHDA formed 2 : 1 pairs with 4Bpy, resulting in stable monolayers. The bright rows correspond to pyrene groups of PHDA. The darker rows correspond to the alkyl chains, which were aligned with the graphite in the same way as the uni-component monolayers. The 4Bpy molecule was observed as two bright spots in the STM image and it formed hydrogen bonds with two PHDA molecules. Two PHDA molecules in the bordering rows coupled with pyrene moieties, congregated at the brightest rows. In contrast to the uni-component monolayers, the individual pyrene unit was not clearly identified as a ring structure. A similar structural change upon the addition of 4Bpy has been observed in the system of 4Bpy and a simple fatty acid like stearic acid.[24,25] Therefore, the structural change is probably due to the formation of a hydrogen bond between the carboxyl group and 4Bpy, and not directly affected by interactions between aromatic units. According to our structural analysis, the planes of the pyrene units were deduced to be tilted at an angle of *ca*. 30 degrees with respect to the graphite surface, whereas the pyrene units in the same row overlapped each other. We consider that π–π interaction would be strong between overlapped pyrene units. This would be one of the possible reasons why the individual pyrene moieties were not clearly observed in these STM images. The proposed space-filling model of the packing structure is illustrated in Fig. 3c.

Periodically disordered lamellas were observed only with a high concentration of 4Bpy and low temperatures, as mentioned above. In this lamella, PHDA with 4Bpy formed a pair (Structure III) as shown in the STM images (Figs. 3 and 4) and illustrated in the corresponding model (Fig. 5). In the disordered lamella near the domain boundary, domino-like molecular motions of individual PHDA molecule were observed with

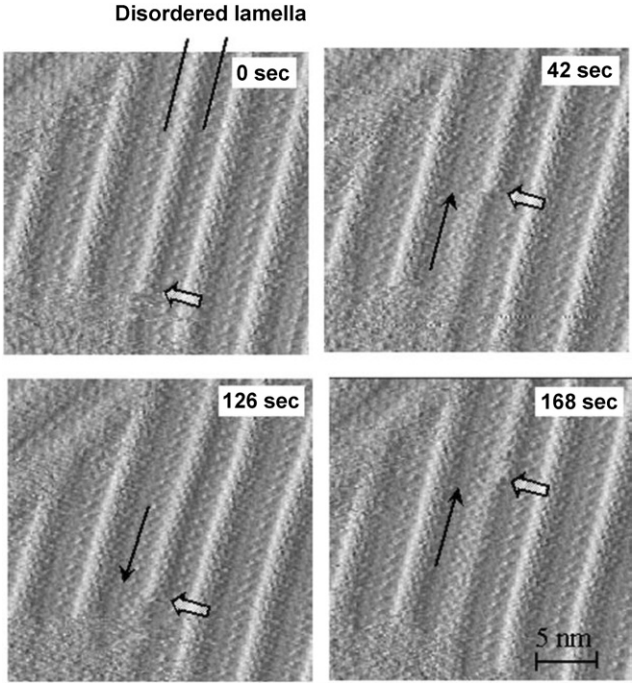

Fig. 4 A series of STM images of the same area of 1-PHDA and 4Bpy co-adsorbed monolayers at $t = 0$ s, $t = 42$ s, $t = 126$ s, and $t = 168$ s. The arrows indicate the position where 1-PHDA molecules changed their orientation. Image sizes are 25×25 nm^2 (bias: 1.0 V (sample negative), tunneling current: 0.35 nA, with the constant height mode).

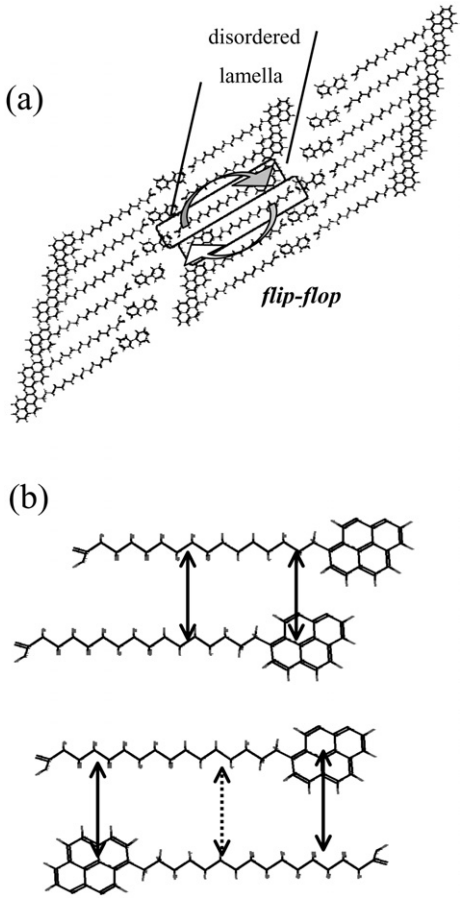

Fig. 5 (a) Proposed assembled structure and molecular re-orientation in the disordered lamella. (b) Schematic illustration of the molecular interactions for the parallel (top) and anti-parallel orientation (bottom).

the STM. Fig. 4 depicts a series of STM images showing the motions with sub-molecular resolution. At 0 seconds, all of the PHDA molecules in the disordered row oriented their pyrene moieties to the right. After 42 s, a clear structural change was observed from the lower side to the middle of the STM image in the row. Here, *ca*. 8 molecules had changed their orientation by 180°. In the STM image, the arrow indicates the position of the orientation defect of PHDA. These molecules flipped after 126 s and re-oriented again after 168 s. This structural fluctuation continued for more than a few hours until the domain disappeared due to growth of another domain.

The scan direction of an STM probe could have affected such desorption–adsorption processes in principle. The employed STM collects images by scanning alternately from top to bottom and from bottom to top. For example, the image at 0 seconds was obtained by scanning from bottom to top of the image, and the next image after 42 s was from top to bottom in Fig. 4. Fig. 6 shows the time dependence of the re-orientation in the disordered row. The graph shows the change in the distance between the defect position of the orientation and the domain boundary at the bottom of the images shown in Fig. 4 as a function of time. Fig. 6 indicates, however, that the scan direction did not directly correlate with the structural fluctuation of the PHDA molecules. Therefore, we consider that the observed re-orientation was not driven by the probe scanning.

It should be noted that this molecular re-orientation occurred only in a disordered row without any disordering and re-orientation of the other assembled structures. The structural fluctuation was related to the desorption–adsorption process and initiated at the domain boundary due to the instability of adsorption near the boundary. Interestingly, the

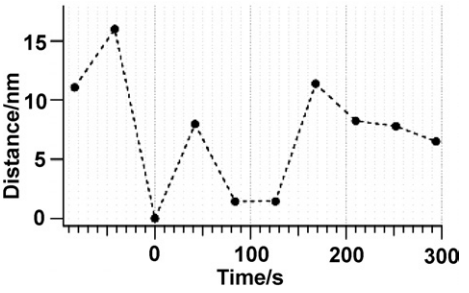

Fig. 6 The position of the orientation defect as a function of time in the single disordered row. The plot shows changes in the distances between the point of anti-parallel configuration and the domain boundary at the bottom of the STM image shown in Fig. 4. The scan directions at −42, 42, 126, 210, 294 s were top-to-bottom and that at −84, 0, 84, 168, 252 s were bottom-to-top of the image.

anti-parallel defect configuration sometimes moved in the range of hundreds of nanometers along the row, but we were hardly ever able to find more than one defect in the same row. The process can be called a co-operative phenomenon, since PHDA molecules have a tendency to get orientated in the same direction with neighbour molecules in the single row. It is interesting that each PHDA molecule did not change its orientation independently and randomly with respect to the neighbour molecules, whereas each PHDA molecule within the disordered row seems to have the same interaction with the two bordering rows irrespective of its orientation. This is because the disordered row is sandwiched between two bordering rows, being forced to interact with the pyridine groups from both sides. This situation is illustrated in Fig. 5a.

In order to explain the co-operative molecular motion in the disordered row, we compared the lateral interaction between PHDA molecules in two orientations (parallel and anti-parallel), as illustrated in Fig. 5b. We neglected the hydrogen bonding with 4Bpy in the neighbouring rows for the reason mentioned above. When PHDA molecules are oriented in the same direction with the neighbour molecule as in the upper part of Fig. 5b (parallel), the interactions are considered to be dominated by 2 factors, *i.e.* the interaction between two pyrene units and the interaction between two alkyl chains. In the case of the opposite orientation, as shown in the bottom part of Fig. 5b (anti-parallel), the possible interactions are between alkyl chains as well as between a pyrene unit and an alkyl chain. We assumed that the interaction between the pyrene unit and the alkyl chain could be neglected in the latter case since the distance between them is larger than the former case so that the interaction should be weak. The interaction energies have been estimated to be 5 kJ mol^{-1} per CH_2 unit between alkyl chains and 18 kJ mol^{-1} between pyrene units on the basis of the crystal sublimation enthalpy[26] and theoretical calculations.[27] Then, the total attractive forces can be estimated to be 43 kJ mol^{-1} and 20 kJ mol^{-1} for the parallel and anti-parallel orientations, respectively. This estimation clearly indicates that the parallel orientation is more favorable than the anti-parallel one. The difference is mainly ascribable to the interaction between the pyrene units. Therefore we conclude that the π–π interaction is the most important factor leading to the observed cooperative molecular motion.

The observed cooperative structural fluctuation sometimes occurred over a large range (> 100 nm) and continued without disordering other regions for a few hours, which was limited only by the growth of other domains or by experimental limitations of STM measurements due to solvent evaporation. This means that the disordered lamella is rather stable as a phase, having bistability so as to undergo a structural fluctuation. The cooperative motion can be associated with the Ising model for describing the magnetic characteristics of one-dimensional spin systems where the parallel orientation

is more stable than the anti-parallel one. The model predicts that all spins are oriented towards the same direction at a low temperature, and the orientation randomness among spins increases with temperature. In the present system, the large-scale fluctuation was observed only in a limited temperature range because an increase in orientation randomness leads to instability of the lamella structure itself at the liquid–solid interface. Large-scale concerted fluctuations may exist in many molecular assembled systems, including biological systems, and may play an important role in these systems' functions.

Conclusion

In this work, we investigated the static and dynamic properties of self-assembled monolayers of PHDA. In the uni-component monolayers of PHDA, the molecule formed a stable packing structure and no dynamic process was observed except near the domain boundary. The pyrene group of the corresponding molecule was observed as a bright ring in the STM images and its shape was similar to the electron densities of HOMO and LUMO levels. A drastic structural change within the self-assembly induced by the co-adsorption with 4Bpy, was observed. In the co-adsorbed monolayers, the pyrene units overlapped each other. At a low temperature and high concentration of 4Bpy, bistable structures were observed in the monolayers. In these structures, domino-like cooperative molecular motions were observed with time-lapsed STM measurements. The cooperative structural fluctuation is considered to be dominated by the π–π interaction between the pyrene units. An increase in the contrast of the pyrene groups caused by their overlapping was found and further studies are underway.

Acknowledgements

This work was supported by a Grant-in-Aid for Scientific Research from the Japanese Ministry of Education, Science, Sports and Culture (11355035, 13440204).

References

1 G. C. McGonigal, R. H. Bernhardt and D. J. Thomson, *Appl. Phys. Lett.*, 1990, **57**, 28.
2 J. P. Rabe and S. Buchholz, *Science (Washington. D. C.)*, 1991, **253**, 424.
3 B. Venkataraman, G. W. Flynn, J. L. Wilbur, J. P. Folkers and G. M. Whitesides, *J. Phys. Chem.*, 1995, **99**, 8684.
4 S. De Feyter, P. C. M. Grim, M. Rücker, P. Vanoppen, C. Meiners, M. Sieffert, S. Valiyaveettil, K. Müllen and F. C. De Schryver, *Angew. Chem. Int. Ed.*, 1998, **37**, 1223.
5 D. G. Yablon, J. Guo, D. Knapp, H. Fang and G. W. Flynn, *J. Phys. Chem.*, 2001, **105**, 4313.
6 L. Askadskaya and J. P. Rabe, *Phys. Rev. Lett.*, 1992, **69**, 1395.
7 B. Venkataraman, J. J. Breen and G. W. Flynn, *J. Phys. Chem. B*, 1995, **99**, 6608.
8 A. Stabel, R. Heinz, F. C. De Schryver and J. P. Rabe, *J. Phys. Chem.*, 1995, **99**, 505.
9 M. Hibino, A. Sumi and I. Hatta, *Jpn. J. Appl. Phys.*, 1995, **34**, 3354.
10 M. Hibino, A. Sumi and I. Hatta, *Thin Solid Films*, 1996, **281–282**, 594.
11 A. Gesquiere, M. M. Abdel-Mottaleb, S. De Feyter, F. C. De Schryver, M. Sieffert, K. Müllen, A. Calderone, R. Lazzaroni and J. L. Bredas, *Chem. Eur. J.*, 2000, **6**, 3739.
12 A. Stabel, R. Heinz, J. P. Rabe, G. Wegner, F. C. De Schryver, D. Corenes, W. Dehaen and C. Suling, *J. Phys. Chem.*, 1995, **99**, 8690.
13 D. F. Padowitz and B. W. Messmore, *J. Phys. Chem. B*, 2000, **104**, 9943.
14 D. F. Padowitz, D. M. Sada, E. L. Kemer, M. L. Dougan and W. A. Xue, *J. Phys. Chem. B*, 2002, **106**, 593.
15 J. Cousty and L. P. Van, *Phys. Chem. Chem. Phys.*, 2003, **5**, 599.
16 L. C. Giancarlo and G. W. Flynn, *Acc. Chem. Res.*, 2000, **33**, 491.
17 S. De Feyter, A. Gesquiere, M. M. Abdel-Mottaleb, P. C. M. Grim, F. C. De Schryver, C. Meiners, M. Sieffert, S. Valiyaveettil and K. Müllen, *Acc. Chem. Res.*, 2000, **33**, 520.
18 A. Ulman, *Acc. Chem. Res.*, 2001, **34**, 855.
19 S. De Feyter, J. Hofkens, M. Van der Auweraer, R. J. M. Nolte, K. Müllen and F. C. De Schryver, *Chem. Commun.*, 2001, 585.
20 E. Mena-Osteritz, *Adv. Mater.*, 2002, **14**, 609.
21 R. E. Palmer and Q. Guo, *Phys. Chem. Chem. Phys.*, 2002, **4**, 4275.
22 A. Hoshino, S. Isoda, H. Kurata and T. Kobayashi, *J. Appl. Phys.*, 1994, **76**, 4113.
23 T. Ogawa, S. Irie, S. Isoda, T. Kobayashi and M.-H. Whangbo, *Jpn. J. Appl. Phys.*, 1998, **37**, 3864.
24 P. Qian, H. Nanjo, T. Yokoyama, T.M. Suzuki, K. Akasaka and H. Orhui, *Chem. Commun.*, 2000, 2021.
25 B. Xu, S. Yin, C. Wang, Q. Zeng, X. Qui and C. Bai, *Surf. Interface Anal.*, 2001, **32**, 245.
26 *Handbook of Chemistry and Physics*, 1989–1990, 70th edn., C-664.
27 S. Tsuzuki, T. Uchimura, K. Matsumura, M. Mikami and K. Tanabe, *Chem. Phys. Lett.*, 2000, **319**, 547.